Food and Chemical Toxicology 134 (2019) 110806

Contents lists available at ScienceDirect

Food and Chemical Toxicology

journal homepage: www.elsevier.com/locate/foodchemtox

Effects and mechanisms of iridoid glycosides from *Patrinia scabiosaefolia* on improving insulin resistance in 3T3-L1 adipocytes

Zhenhua Liu[a,b,1], Lanting Xu[a,c,1], Xiaoqing Xu[b,c], Yun Niu[a,b], FatmaS.A. Saadeldeen[b,c], Wenyi Kang[a,b,*]

[a] National R & D Center for Edible Fungus Processing Technology, Henan University, Kaifeng, 475004, China
[b] Joint International Research Laboratory of Food & Medicine Resource Function, Henan Province, Henan University, Kaifeng, 475004, China
[c] Kaifeng Key Laboratory of Functional Components in Health Food, Kaifeng, 475004, China

ARTICLE INFO

Keywords:
Patrinoside
Patrinoside A
Insulin resistance
PI3K
p-Akt
GLUT4

ABSTRACT

Insulin resistance causes several adverse effects such as hypertension, diabetes and different aspects of cardiovascular diseases. *Patrinia scabiosaefolia* Fisch. ex Trev. is a traditional Chinese edible herbal, whose *n*-BuOH extract significantly increased glucose transportin 3T3-L1 adipocytes at the concentration of 12.5 μM. To determine its active constituent, its chemical components and bioactivities were investigated. Two compounds (**1**–**2**) could significantly improve insulin resistance in 3T3-L1 adipocytes at concentrations around 25.0 μM ($P < 0.001$). Compound **2** was more effective to lower the content of glucose content at 12.5 μM ($P < 0.001$). Compound **1** was a new compound identified by spectroscopic methods. Western-blot experiment demonstrated an upregulation of p-IRS-1, p-Akt, and GLUT4 induced by compounds **1** and **2**. Hence, we speculated that compounds **1** and **2** could activate PI3K and Akt signaling by up-regulating of p-IRS-1 which resulted in the activation of PI3K before phosphorylating Akt, ultimately led to translocation of GLUT4. These events finally improve glucose transport. Our results may provide the scientific basis for the development and effective use of *P. scabiosaefolia* against type 2 diabetes.

1. Introduction

Insulin represents the main regulatory hormone of glycolipid metabolism. In conditions of insulin resistance (IR), the biological effects of insulin on the target organs and tissues are reduced or lost, resulting in varieties of pathological phenomenon (Roy, 2012). It is well accepted that long-term insulin resistances could cause a series of adverse reactions in the body, such as hypertension, diabetes and cardiovascular diseases (Cederberg and Enerbäck, 2003).

Pharmacological studies showed that the reason for insulin resistance can be roughly divided into three categories: (1) pre-receptor factors, for instance mutation of insulin-related genes, increased titers of antibodies against insulin or degradation of insulin (Bi, 2014; Caruso et al., 2014); (2) receptor factors, leading to obstruction of insulin signaling as indicated by either reduce numbers and affinities of insulin receptor (Ins R), decrease activity of protein tyrosine kinase (PTK) or impaire phosphorylation of insulin receptor β subunit (Bonala et al., 2014); (3) post-receptor factors, including impairment of associated signal proteins involved in signal transduction by mechanisms of phosphorylation (Lei, 2013). Binding of insulin to its receptor first activates the β-subunit of PTK. As a docking protein, insulin receptor substrate (IRS) then binds to a signal molecule containing the Src-homology 2 domain (SH2) which is activated through at least two signaling pathways: 1) activation of phosphatidylinositide-3 kinase (PI3K) pathway by IRS. 2) activation of mitogen-activated protein kinase (MAPK) pathway via Grb2/SOS and RAS proteins, demonstrated to induce inflammation (Cusi et al., 2000; Pessin and Saltiel, 2000).

Several studies have been shown that the PI3K insulin signaling pathway plays an important role in the development of IR. Predominantly, insulin binds to IRS, resulting in tyrosine

Abbreviations: Akt, serine-threonine kinase; HSQC, Heteronuclear singular quantum correlation; HMBC, ^{1}H detected heteronuclear multiple bond correlation; IRS, insulin receptor substrate; IR, insulin resistance; Ins R, insulin receptor; IR, Infrared Radiation; GLUT4, glucose transporter 4; MAPK, mitogen-activated protein kinase; NMR, Nuclear Magnetic Resonance; PTK, protein tyrosine kinase; PI3K, phos-phatidylinositide-3 kinase; *P. scabiosaefolia*, *Patriniascabiosaefolia*; SH2, Src-homology 2 domain; TCM, traditional Chinese medicines

* Corresponding author. National R & D Center for Edible Fungus Processing Technology, Henan University, Kaifeng, China.
E-mail address: kangweny@hotmail.com (W. Kang).

[1] These authors contributed equally to this work.

https://doi.org/10.1016/j.fct.2019.110806
Received 9 August 2019; Received in revised form 30 August 2019; Accepted 5 September 2019
Available online 12 September 2019
0278-6915/

phosphorylation of IRS in fat cells. Phosphorylated IRS activates its catalytic subunit p110 of PI-3K through binding to its regulatory subunit p85 (Alghamdi et al., 2014). Finally, PI3K phosphorylates serine-threonine kinase of Akt. Activation of Akt affects the translocation of glucose transporter (mainly GLUT4). Insertion of GLUT4 by insulin thus leads to an increased import of glucose (Jane et al., 2012; Rea and James, 1997). Knock out experiments revealed the importance of PI3K leading to diabetic conditions (Kadowaki, 2000). Similarly, knocking out Akt led to reduced glycogen in the liver or absorption of blood sugar in the skeletal muscles (Cho, 2001). In another study, it had been demonstrated that a decrease of GLUT4 protein, insulin receptor substrate (IRS1, IRS2), and the p85 of PI-3K could influence the glucose transport in adipocytes (Zhang, 1997). The importance of the PI3K pathway resulting in IR had been demonstrated (Cao et al., 2011; Nishida et al., 2009; Takenaka et al., 2009; Zhang et al., 2010).

Currently, there are mainly two types of drugs used to improve IR: hypoglycemic agents, such as sulfonylureas, biguanides, α-glucosidase inhibitors and lipid-lowering agents, for instance fibrates and nicotinic acid (Stumvoll et al., 1990; Saltiel and Olefsky, 1996). However, all these drugs may have adverse effects, such as gastro-intestinal reactions, hepatotoxicity, or others (Meng, 2013). Recent studies using traditional Chinese medicines (TCM) demonstrated prominent effect in improving IR, and single molecules from Chinese medicinal herbs had been isolated as their active ingredients (Chen and Huang, 2016; Zhu, 2015). TCM usually show multi-targets effects to improve IR. Currently, their mechanisms remain unknown. Therefore, it is very important to determine active constituents from TCM and explore their mechanisms leading to improved IR.

Previously, our group showed increased glucose transport by the crude extract of traditional Chinese medicine (Xu et al., 2019). ex Trev. And we found the EtOAc extract and n-BuOH extract of *Patrinia scabiosaefolia* Fisch. ex Trev. could significantly improve glucose consumption in adipocytes ($P < 0.01$, $P < 0.001$ respectively) at 12.5 μM. Hence, we systematically explored the bioactive constituents of *P. scabiosaefolia*. As a result, two compounds (**1–2**) (Fig. 1) were isolated and identified, including a new compound (**1**) and the known compound patrinoside (**2**), both showed significant activities against IR in 3T3-L1 cells. We discussed the effects of compounds **1** and **2** by mechanisms of the PI3K pathway, as indicated by an upregulation of PI3k, p-IRS-1, p-Akt and GLUT4. Our study may provide the scientific basis for the development and effective use of *P. scabiosaefolia* against insulin resistance.

2. Materials and methods

2.1. General experimental procedures

Optical rotation was obtained on a JASCO P-1020 digital polarimeter (Horiba, Tokyo, Japan). UV spectra were measured by a Shimadzu UV-2401 PC spectrophotometer (Shimadzu, Kyoto, Japan). IR spectra were obtained on a Bruker Tensor 27 infrared spectrophotometer (Bruker Optics GmbH, Ettlingen, Germany) with KBr pellets. Mass spectra were performed on an API QSTAR time-of-flight spectrometer (MDS Sciqaszex, Concord, Ontario, Canada) and LCMS-IT-TOF (Shimadzu, Kyoto, Japan) spectrometer. NMR spectra were recorded on Bruker Ascend TM 400 superconducting NMR spectrometer with TMS as the internal standard (BrukerCo., Germany). The chemical shifts were given in δ (ppm) with reference to the solvent signal. Column chromatography was performed on silica gel (200–300 mesh, Qingdao Ocean Chemical Co., Ltd., Qingdao, Shandong, China), Lichroprep Rp-18 gel (40–63 μm, Merck, Darmstadt, Germany), Sephadex LH-20 (Pharmacia Co., Sweden), YMC*GEL ODS-A-HG (50 μm, YMC Co. Ltd. Japan).

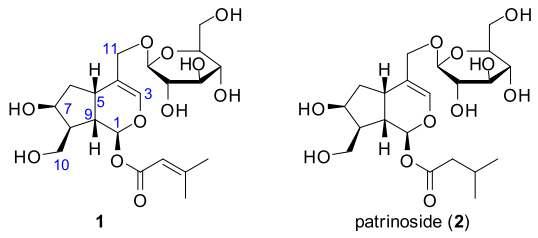

Fig. 1. The chemical structures of compound **1** and patrinoside (**2**).

2.2. Extraction and isolation

The plants of *P. scabiosaefolia* were collected in September 2017 from DuYun City, Guizhou Province. The material was identified by Prof. Chang-Qin Li at Henan University and a voucher specimen (20170909) was deposited at Joint International Research Laboratory of Food & Medicine Resource Function.

The dried and powdered whole plants (5 kg) of *P. scabiosaefolia* were extracted with 95% ethanol under room temperature and concentrated under reduced pressure. Then, the extract was partitioned with EtOAc and *n*-BuOH successively, yielding EtOAc extract (150 g) and *n*-BuOH extract (210 g) after concentration. The *n*-BuOH extract (210 g) was separated by silica gel column chromatography, reversed phase C-18 column chromatography, Sephadex LH-20 column chromatography to obtain compounds **1** and **2**.

PatrinosideA (1):Light yellow oil; [α]24 D-69.5 (*c* 0.03, MeOH); UV (MeOH) λ_{max} (log ε): 218 (4.23) nm; IR (KBr) ν_{max} 3416, 2924, 2885, 1725, 1646, 1127 cm^{-1}; ^1H and ^{13}C NMR data, see Table 1; positive ESIMS *m/z* 483 $[M + Na]^+$;HREIMS *m/z*483.1836 $[M + Na]^+$ (calcd.483.1837 for $C_{21}H_{32}O_{11}Na$).

Patrinoside (2): Light yellow oil; [α]24 D-16.7 (*c* 0.03, MeOH); UV (MeOH) λ_{max} (log ε): 205 (3.38) nm; IR (KBr) ν_{max} 3423, 2927, 2885, 1741, 1632, 1077 cm^{-1}; ^1H and ^{13}C NMR data, see Table 1; positive ESIMS *m/z* 485 $[M + Na]^+$; HREIMS *m/z* 485.1995 $[M + Na]^+$ (calcd.485.1993 for $C_{21}H_{34}O_{11}Na$).

2.3. Cell culture

Mouse 3T3-L1 preadipocytes (Cobioer, Nanjing, China) were

Table 1
The ^1H and ^{13}C-NMR data of compounds **1** and **2** (δ in ppm, *J* in Hz) in CD_3OD.

Position	1		2	
	δ_H	δ_C	δ_H	δ_C
1	5.90 (d, 5.4)	93.2	5.90 (d, 5.4)	93.6
3	6.37 (s)	140.2	6.37 (s)	140.1
4	–	116.4	–	116.4
5	3.03 (q, 7.8)	34.2	3.01 (q, 7.9)	34.1
6	2.07 (m)	40.9	2.06 (m)	40.9
	1.82 (m)		1.83 (m)	
7	4.32 (m)	73.3	4.32 (m)	73.3
8	1.95 (m)	49.2	1.94 (m)	49.1
9	2.18 (m)	42.7	2.17 (m)	42.7
10a	3.80 (dd, 7.6, 11.0)	62.2	3.80 (dd, 7.5, 11.0)	62.2
10b	3.72 (dd, 5.6, 11.0)		3.71 (dd, 5.7, 8.7)	
11a	4.26 (d, 11.5)	69.8	4.26 (d, 12.2)	69.7
11b	4.08 (d, 11.5)		4.08 (d, 11.5)	
1′	–	166.4	–	173.4
2′	5.70 (t-like, 1.3)	116.2	2.23 (dd, 1.9, 7.5)	44.1
3′	–	161.0	2.07 (m)	26.8
4′	1.93 (d, 1.1)	27.6	0.96 (d, 6.7)	22.6
5′	2.17 (d, 1.1)	20.6	0.96 (d, 6.7)	22.6
1″	4.28 (d, 7.8)	103.4	4.28 (d, 7.9)	103.4
2″	3.19 (m)	75.1	3.18 (m)	75.1
3″	3.26 (m)	77.9	3.26 (m)	77.9
4″	3.26 (m)	71.7	3.26 (m)	71.7
5″	3.35 (m)	78.1	3.34 (m)	78.1
6″a	3.86 (dd, 2.0, 11.9)	62.8	3.86 (dd, 2.0, 12.1)	62.8
6″b	3.66 (dd, 5.5, 11.9)		3.65 (m)	

cultured in DMEM high glucose mediumsupplemented with 15% fetal bovine serum (FBS) and penicillin (100 U/mL)-streptomycin (100 μg/mL) mixture in a 37 °C, 5% CO_2 incubator for culture until the cell confluency reached 70%–80%.

2.4. Cell viability assay

3T3-L1 preadipocytes were seeded into 96-well plates at a density of 5×10^3 cells per well and cultured for 24 h. Cells were treated with different concentrations of compound **1** or **2** for 48 h. Then, MTT (0.5 mg/ml) was added to keep 37 °C for 4 h. The resultant formazan was dissolved in DMSO (100 μL/well) and measured at OD_{492} by a microplate spectrophotometer (Thermo Fisher, Finland).

2.5. Treatment of IR 3T3-L1 adipocytes

After cell contact inhibition, medium was changed to 10% FBS DMEM supplemented with 0.5 mM 3-isobutyl-1methylxanthine, 1 mM dexamethasone (Dex) and 10 μg/ml insulin.3 days later, the medium was replaced with DMEM supplemented with insulin (10 μg/mL) for 2 d and changed to normal culture medium and cultured for another for 4 d. After inducing differentiation into mature adipocytes, 1 μM Dex was used for modeling for 72 h. Sodium Orthovanadate (Van, Alfa Aesar M30D004) was used as a positive control and given different concentrations of compound **1** or **2** for 48 h. Glucose oxidase-peroxidase (GOD-POD) method was used to determine the level of glucose in the cell supernatant used a glucose assay kit (Shanghai Rongsheng Biotech Co) according to the manufacturer's instructions.

2.6. Western blot analysis

Cells harvested with different concentrations of compound 1 or 2 for 48 h were collected and lysed on ice for 30 min in a mixture containing Radio-Immunoprecipitation Assay (RIPA), phenylmethane sulfonyl fluoride (PMSF), and phosphatase inhibitors. The lysate was centrifuged at 12,000 rpm for 10 min at 4 °C. Protein concentration was measured by a BCA protein assay kit (Solarbio Science & Technology Co., Beijing, China). Protein samples at same amount (70 μg) were separated on 10% SDS polyacrylamide gel. Proteins were transferred onto polyvinylidene fluoride membranes (PVDF) (0.2 μM, EMD Millipore, MA, USA), which were blocked in 5% nonfat dry milk in Tris-buffered saline with 1% Tween 20 (TBS-T, Solarbio, Beijing, China) for 2 h. Then, the PVDF membrane was incubated with the primary antibody overnight at 4 °C. Then, it was incubated with horseradishperoxidase conjugated secondary antibody for 1 h. After washing, protein bands were visualized by enhanced chemiluminescence (ECL, Solarbio, Beijing, China) and an imaging system (ProteinsiMple FluorcheM Q) according to the manufacturer's instructions.

2.7. Statistical analysis

The experimental results were analyzed by SPSS 19.0 software. The results are shown as means ± standard deviation (SD). *P* values less than 0.05 were considered statistically significant.

3. Results

3.1. Identification of compound 1

Compound **1** was obtained as light yellow oil. The HRESI spectrum displayed a quasi-molecular iron at *m/z* 483.1836 $[M + Na]^+$ (calcd. 483.1837), consistent with the chemical formula $C_{21}H_{32}O_{11}$, and its infrared spectroscopy displayed absorptions due to hydroxyl groups at 3416 cm^{-1}, carbonyl groups at 1725 and 1646 cm^{-1}. Analysis of the ^1H, ^{13}C NMR and HSQC spectra (Table 1) revealed two methyl groups, four methenes, twelve methines and three quaternary carbons. Further analysis of the ^{13}C NMR and HMBC spectra led to find a 3-methylcrotonyl residue atδ_C 166.4 (s), δ_C 116.2 (s), δ_C 161.0 (d), δ_C 27.6 (q), δ_C 20.6 (q) with δ_H 1.93 (d, J = 1.1 Hz) and δ_H 2.17 (d, J = 1.1 Hz), as well as a *β*-D-glucopyanosyl moiety at δ_C 103.4 (d), δ_C 75.1 (d), δ_C 77.9 (d), δ_C 71.7 (d),δ_C 78.1 (d), δ_C 62.8 (t) with δ_H 4.28 (d, J = 7.8 Hz, H-1″). Thus, there remained ten carbons, including a hemiketal methine at δ_H 5.90 (d, J = 5.4 Hz, H-1) and δ_C 93.2 (d, C-1), a trisubstituted olefinic bond at δ_H 6.37 (s, H-3), δ_C 140.2 (d, C-3), and δ_C 116.4 (s, C-4), two oxygenated methenes at δ_C 62.2 (t, C-10) and δ_C 69.8 (t, C-11), and a oxymethine at δ_C 73.3 (C-7). Besides, extensive analysis of the COSY spectrum enabled the coupling sequences of C (1)-C (9)-C (5)-C (6)-C (7)-C (8)-C (10). These data clearly suggested **1** to be a valeriana-type iridoid, namely, the dihydropenstemide (Boros and Stermitz, 1991; Gering et al., 1986) The HMBC correlations from H-1 (δ_H 5.90) to C-1' (δ_C 166.4), and the H-11 (δ_H 4.26, 4.08) to C-1" (δ_C 103.4) suggested that the 3-methylcrotonyl group should be placed at C-1, and the glucose was located at C-11.

The stereo-configuration of **1** was acquired by the ROESY and CD spectra, as well as the coupling constant. The ROESY correlations of H-1 with H-7 and H-8 suggested the *α*-orientation of H-7 and H-8. Similarly, the relative configuration of H-5 was *β*-orientation deduced by the correlations from H-9 to H-5 in the ROESY (Fig. 2). There is a good agreement between compound **1** and patrinoside (**2**) in the ECD spectra which indicate that the absolute configuration of **1** was the same as patrinoside (Fig. 3), whose configuration was determined by X-Ray crystallographic analysis (Taguchi, 2008), on account of the structural similarity between **1** and patrinoside (**2**). In addition, the coupling constant $J_{1'',2''}$ = 7.8 Hz suggested a *β* glycosidic linkage at C-11. Thus, the structure of **1** was established as (1*S*,5*S*,7*S*,8*S*,9*S*)-1-*O*-(3-methylcrotonyl)-7,10-dihydroxy-11-*β*-D-glucose-5,6-dihydrovaltrate hydrin, named as patrinoside A.

3.2. Effects of the extract from P. scabiosaefolia on glucose depletion in IR adipocyte

The effects of the EtOAc extract and *n*-BuOH extract on insulin sensitivity in 3T3-L1 adipocyte were assessed by cellular glucose uptake analysis. Compared with the control vehicle group, the treatment group significantly reduced the sugar uptake of adipocytes ($P < 0.001$), confirming the successful establishment of the insulin resistance model. The EtOAc extract and *n*-BuOH extract could significantly improve glucose consumption in adipocytes with $P < 0.01$ and $P < 0.001$ at the consebntration of 12.5 μM compared with the model group (Fig. 4).

3.3. Effects of compounds 1 and 2 on viability of 3T3-L1 cell

The MTT assay was used to evaluate the cytotoxicity of compounds **1** and **2** in 3T3-L1 adipocytes. Compounds **1** and **2** showed no significant cytotoxicity at concentration at 100 μM (Fig. 5). Therefore, the concentrations from 12.5 to 100 μM were used in the subsequent.

3.4. Effects of compounds 1 and 2 on glucose depletion in IR adipocyte

The effects of compounds **1** and **2** on insulin sensitivity in 3T3-L1

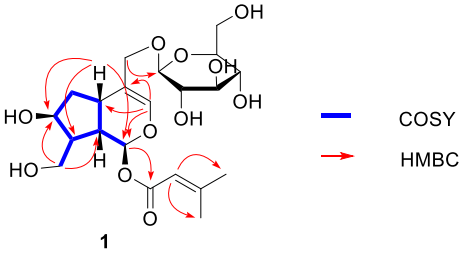

Fig. 2. Key ^1H–^1H COSY and ^1H–^{13}C HMBC correlations of compound **1**.

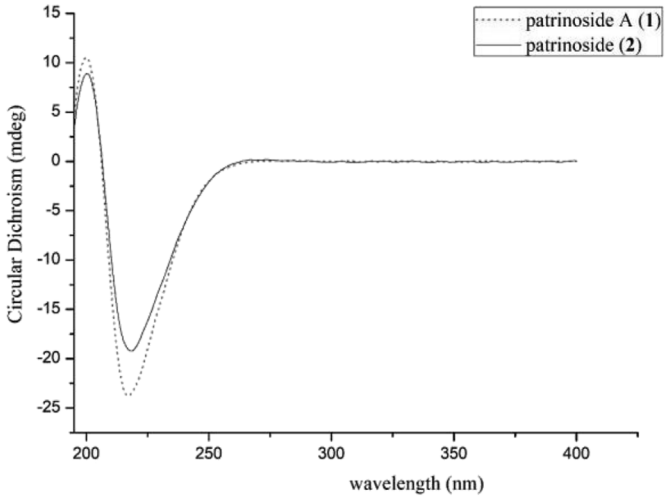

Fig. 3. ECD spectra of compounds **1** and **2** at the TDDFT/B3LYP/6-31G(d) level.

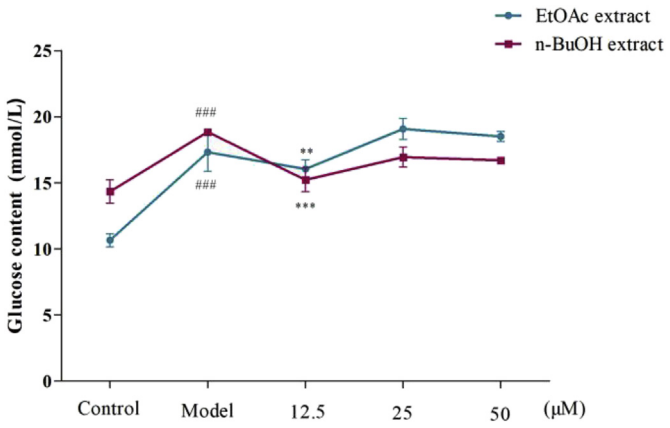

Fig. 4. Effects of EtOAc extract and *n*-BuOH extract on glucose consumption in IR adipocytes. After Dex treatment of adipocytes for 72 h, given different concentrations of EtOAc extract and *n*-BuOH extract for 48 h. Determination of glucose levels in cell supernatants using a glucose assay kit. Data are presented as means ± SD, $n = 6$. ***P < 0.001,**P < 0.01 versus control group, $^{###}P < 0.001$ versus model group.

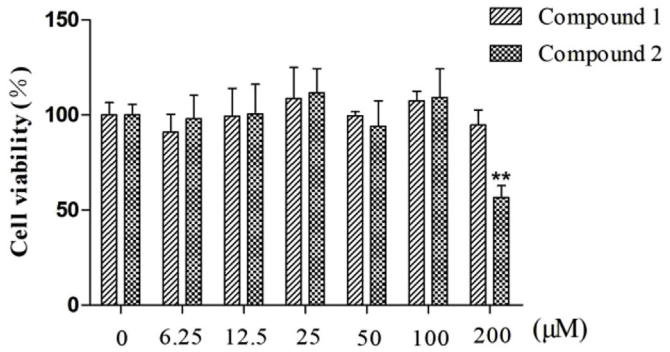

Fig. 5. Effects of compounds **1** and **2** on the viability of 3T3-L1 adipocytes. Measurement of cell viability using MTT after giving different concentrations of compound **1** or **2** for 48 h. Data arepresented as means ± SD, $n = 6$. $^{**}P < 0.01$ versus control group.

adipocyte were assessed by the cellular glucose uptake assay. Compared with the control vehicle group, the Dexamethasone treatment group significantly reduced the sugar uptake of adipocytes confirming the successful establishment of the insulin resistance model ($P < 0.001$).

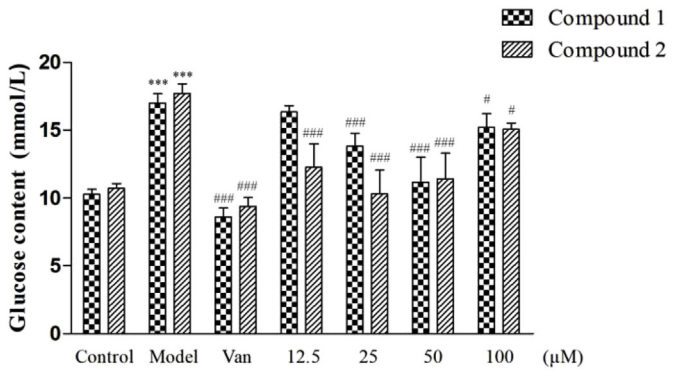

Fig. 6. Effects of compounds **1** and **2** on glucose consumption in IR adipocytes. Dex induced insulin resistance in 3T3-L1 adipocytes. Given different concentrations of compound **1** or **2** for 48 h. Determination of glucose levels in cell supernatants using a glucose assay kit. Data are presented as means ± SD ($n = 6$). $^{***}P < 0.001$ versus control group, $^{#}P < 0.05$, $^{###}P < 0.001$ versusDextreatment group.

Compound **1** significantly improved glucose consumption in adipocytes at concentrations of 25 and 50 μM respectively ($P < 0.001$) compared with Dexamethasone treatment group. Low concentrations (e.g., 12.5 μM) had no significant effects on sugar uptake. As compared to compound **1**, compound **2** lowered glucose at concentrations of 12.5, 25 and 50 μM more effectively ($P < 0.001$). The structures of compounds **1** and **2** were different at C-1. One is a 3-methylcrotonyl residue and the other one is an isovaleryl substituent, which may be responsible for their activities. At concentrations of 50 and 25 μM, compounds **1** and **2** showed strong effects comparable with the positive control (Vanadium) (Fig. 6).

*3.5. Effects of compounds **1** and **2** on PI3K/Akt insulin signaling pathway in 3T3-L1 adipocytes*

In Fig. 7, compounds **1** and **2** (100, 50, and 25 μM) up-regulated the expression of p-IRS-1, p-Akt, GLUT4 in IR 3T3-L1 adipocytes significantly compared with the Dexamethasone treatment group. Compounds **1** and **2** extremely up-regulated the expression of p-IRS-1, p-Akt, and GLUT4 at concentrations of 50, and 25 μM respectively ($P < 0.001$) compared with the positive control (Vanadium). Moreover, compounds **1** and **2** at 50 μM induced a higher expression of p-Akt, GLUT4 compared with vanadium.

4. Discussion

P. scabiosaefolia, a folk medicine in China, is used widely as food for relieving heat and toxic, swelling, apocenosis, promoting blood circulation (Lu and Chen, 1986). In our previous studies, the *n*-BuOH extract of *P. scabiosaefolia* significantly promoted the glucose transport at 12.5 μM in the insulin resistance adipocytes (Fig. 4). To explore its active constituent, two compounds were isolated and identified from the *n*-BuOH extract by varieties of chromatographic materials and extensive spectroscopic methods. Both compounds showed obviously effect to improve glucose consumption in adipocytes (Fig. 6). The new compound **1** and known compound **2** all belong to iridoid glycosides, possessing 7,10,11-trihydroxy-3-en iridoid with ten carbons skeleton and a glucose at C-11. The difference between **1** and **2** is the substituent group at C-1. The former is 3-methylcrotonyl group, and the latter is isovaleryl substituent. It might be the main reason of different activities for two compounds on the glucose depletion in IR adipocytes.

Diabetes is a metabolic and endocrine disease with many cardiovascular complications, becoming a global public health problem (Roy, 2012). Over 90% diabetic is Type 2 Diabetes Mellitus (T2DM), which is characterized by insulin IR (Pang et al., 2004). A number of current

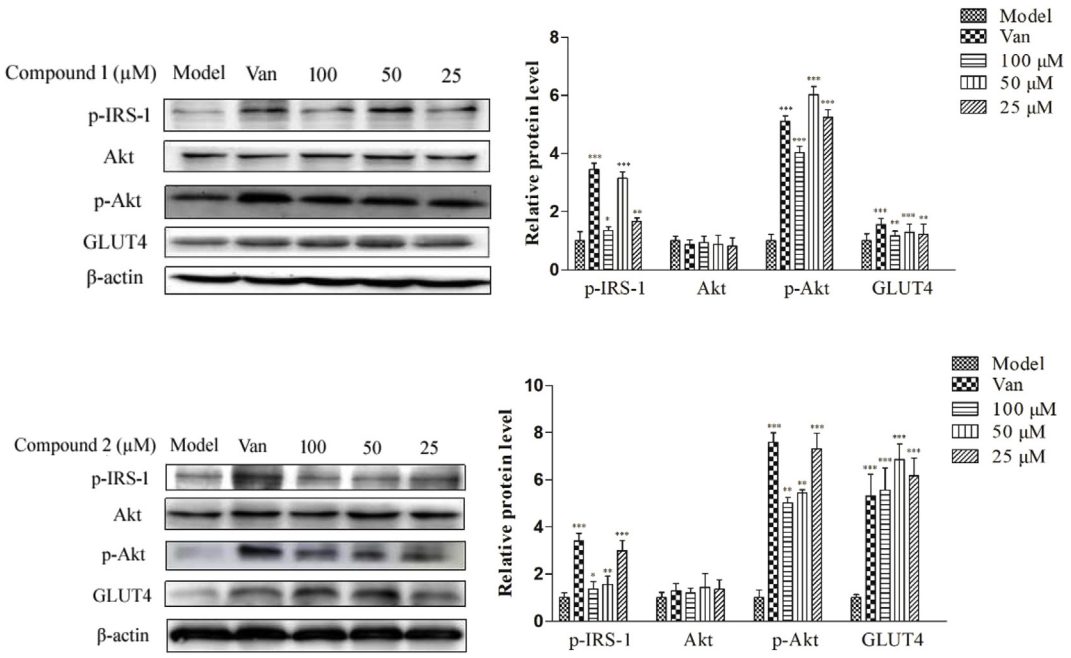

Fig. 7. Compounds **1** and **2** improved glucose uptake in insulin-resistant 3T3-L1 adipocytes through the PI3K/Akt pathway. Different concentrations of Compound **1** and **2** treated insulin-resistant adipocytes for 48 h. Western blot analysis of protein expression of compounds **1** and **2.** Data are presented as means ± SD, $n = 6$. $^{***}P < 0.001$, $^{**}P < 0.01$, $^{*}P < 0.05$ versus Dex treatment group.

studies have shown that IR is mainly caused by the abnormal insulin signal transduction pathways. When insulin binds with its receptor, there are two pathways involved in downstream signal transduction: insulin receptor substrate 1-Rat sarcoma-mitogen activation protein kinase (IRS-RaS-MAPK) and insulin receptor substrate 1-phosphatidylinositol-3 kinase-protein kinase B (IRS-1/PI3K/Akt). The former mainly regulates cell growth and apoptosis while the latter mainly participates in metabolic effects, such as glucose transport and utilization, glycogen synthesis (Guo, 2014; Schinner et al., 2005). Therefore, we detected the expression of proteins related PI3K/Akt signal pathwayfor further mechanisms of improving IR. We found compound **1** up-regulated the expression of p-IRS-1, p-Akt, GLUT4 at concentration of 50 μM and compound **2** also had these effects at concentration of 25 μM (Fig. 7), which suggested that compounds **1** and **2** may work through activating PI3K/Aktsignal pathway. In this pathway, insulin binding in α and β subunits of the insulin receptor activates the tyrosine residues IRS by phosphorylated (Woodruff, 2015). In turn, phosphorylated IRS binds to the p85 regulatory subunit of PI3K and activates its catalytic subunit p110. Activated PI3K phosphorylates serine-threonine kinase (Akt), and activated Akt promotes the GLUT4 translocation from cytosolic to the membrane (Wu et al., 2016). As a result, GLUT4 accelerates the uptake and utilization of glucose in cell (Chi et al., 2014; Gallagher et al., 2012).

According to the literatures and the experimental results, we postulated that the mechanisms of compounds **1** and **2** maybe activate PI3K/Akt signal pathway. The up-regulated expression of p-IRS-1 indicated the activation of IRS, which is important for metabolism of sugar and insulin. Then, phosphorylated IRS activates PI3K, which in turn enhanced the expression of p-Akt agreeing with the experiment. Akt is a downstream PI3K effector and a core protein in the PI3K pathway (Garofalo, 2003). Activated Akt increases the quantity of GLUT4, which was confirmed by the up-regulation of GLUT4. Then, GLUT4 moves from the intracellular pool to the cell membrane, thereby taking part in glucose transport. Thus, compounds **1** and **2** lower the glucose content and improve IR. Therefore, compounds **1** and **2** play the role of improving IR by activating PI3K/Aktsignal pathway.

5. Conclusion

Two compounds were isolated and identified from *P. scabiosaefolia*, including the new described compound **1**. Both compounds had significant effect on improving insulin resistance. Their mechanisms of improving insulin resistance may be exerted via activation PI3K/Akt signaling pathway as indicated by higher expression levels of p-IRS, p-Akt, and GLUT4.

CRediT authorship contribution statement

Zhenhua Liu: Writing - original draft, Data curation. **Lanting Xu:** Writing - original draft, Data curation. **Wenyi Kang:** Writing - original draft.

Declaration of competing interest

The authors declare that they have no known competing financial interests or personal relationships that could have appeared to influence the work reported in this paper.

Acknowledgements

We would like to thank all participants in the study.

Transparency document

Transparency document related to this article can be found online at https://doi.org/10.1016/j.fct.2019.110806

Appendix A. Supplementary data

Supplementary data to this article can be found online at https://doi.org/10.1016/j.fct.2019.110806.

Formatting of funding sources

This work was supported by National Natural Science Foundation of

China (31900292), Science and Technology Development Program of Henan Province (192102110112) and Science and Technology Project of Kaifeng (1908005).

References

Alghamdi, F., Guo, M., Abdulkhalek, S., Crawford, N., Amith, S.R., Szewczuk, M.R., 2014. A novel insulin receptor-signaling platform and its link to insulin resistance and type 2 diabetes. Cell. Signal. 26 (6), 1355–1368.

Bi, Y., Wu, W.J., Shi, J.F., Liang, H., Yin, W.W., Chen, Y.Y., et al., 2014. Role for sterol regulatory element binding protein-1c activation in mediating skeletal muscle insulin resistance via repression of rat insulin receptor substrate-1 transcription. Diabetologia 57 (3), 592–602.

Bonala, S., Lokireddy, S., Mcfarlane, C., Patnam, S., Sharma, M., Kambadur, R., 2014. Myostatin induces insulin resistance via Casitas B-lineage lymphoma b (Cblb)-mediated degradation of insulin receptor substrate 1 (IRS1) protein in response to high calorie diet intake. J. Biol. Chem. 289 (11), 7654–7670.

Boros, C.A., Stermitz, F.R., 1991. Iridoids. An update review, Part II. J. Nat. Prod. 54 (5), 1173–1246.

Cederberg, A., Enerbäck, S., 2003. Insulin resistance and type 2 diabetes–an adipocentric view. Curr. Mol. Med. 3 (2), 107–125.

Caruso, M., Ma, D., Msallaty, Z., Lewis, M., Seyoum, B., Diamond, M., et al., 2014. Increased interaction with insulin receptor substrate 1, a novel abnormality in insulin resistance and type 2 diabetes. Diabetes 63 (6), 1933–1947.

Cusi, K., Maezono, K., Osman, A., Pendergrass, M., Patti, M.E., Pratipanawatr, T., et al., 2000. Insulin resistance differentially affects the PI3-kinase- and MAP kinase-mediated signaling in human muscle. J. Clin. Investig. 105 (3), 311–320.

Cho, H., Mu, J., Kim, J.K., Thorvaldsen, J.L., Chu, Q., Crenshaw, E.B., et al., 2001. Insulin resistance and a diabetes mellitus-like syndrome in mice lacking the protein kinase Akt2 (PKB beta). Science 292 (5522), 1728–1731.

Cao, C., Chen, Y., Wang, W., Liu, Y., Liu, G., 2011. Ghrelin inhibits insulin resistance induced by glucotoxicity and lipotoxicity in cardiomyocyte. Peptides 32 (2), 209–215.

Chen, Y.P., Huang, F., 2016. Research progress on the mechanisms of activeingredients from traditional Chinese medicines intreatment of diabetic insulin resistance. Progress in Pharmaceutical Sciences 40 (3), 197–204.

Chi, M., Ye, Y., Zhang, X.D., Chen, J., 2014. Insulin induces drug resistance in melanoma through activation of the PI3K/Akt pathway. Drug Des. Dev. Ther. 8, 255–262.

Gering, B., Junior, P., Wichtl, M., 1986. Dihydropenstemide from *Penstemon confertus* and the preparation of epi-dihydropenstemidefrom*Penstemide*. Planta Med. 52 (5), 356–358.

Guo, S., 2014. Insulin signaling, resistance, and metabolic syndrome: insights from mouse models into disease mechanisms. J. Endocrinol. 220 (2), T1–T23.

Gallagher, E.J., Fierz, Y., Vijayakumar, A., Haddad, N.G., Yakar, S., Leroith, D., 2012. Inhibiting PI3K reduces mammary tumor growth and induces hyperglycemia in a mouse model of insulin resistance and hyperinsulinemia. Oncogene 31 (27), 3213–3222.

Garofalo, R.S., Orena, S.J., Rafidi, K., Torchia, A.J., Stock, J.L., Hildebrandt, A.L., et al., 2003. Severe diabetes, age-dependent loss of adipose tissue, and mild growth deficiency in mice lacking Akt2/PKBβ. J. Clin. Investig. 112 (2), 197–208.

Jane, G.E., Yvonne, F., Archana, V., Nadine, H., Shoshana, Y., Derek, L., 2012. Inhibiting PI3K reduces mammary tumor growth and induces hyperglycemia in a mouse model of insulin resistance and hyperinsulinemia. Oncogene 31 (27), 3213–3222.

Kadowaki, T., 2000. Insights into insulin resistance and type 2 diabetes from knockout mouse models. J. Clin. Investig. 106 (4), 459–465.

Lei, Z., Tan, I.B., Das, K., Deng, N., Zouridis, H., Pattison, S., et al., 2013. Identification of molecular subtypes of gastric cancer with different responses to PI3-kinase inhibitors and 5-fluorouracil. Gastroenterology 145 (3), 554–565.

Lu, A.M., Chen, S.K., 1986. Delectis Flora Reipublicae Popularis Sinicae Agendae Academiae Sinicae Edita. pp. 007 Flora of China 73(1) Science Press., Beijing, 1986.

Meng, Y.Q., Liu, W.H., Liu, F.X., Zhang, Y., Xue, J., 2013. Research progress on drugs of anti-type 2 diabetes. Drugs & Clinic 28 (3), 461–464.

Nishida, H., Sato, T., Nomura, M., Nakaya, H., 2009. Glimepiride treatment upon reperfusion limits infarct size via the phosphatidylinositol 3-kinase/Akt pathway in rabbit hearts. J. Pharmacol. Sci. 109 (2), 251–256.

Pessin, J.E., Saltiel, A.R., 2000. Signaling pathways in insulin action: molecular targets of insulin resistance. J. Clin. Investig. 106 (2), 165–169.

Pang, J.H., Zhou, Y., Wang, Z.J., 2004. Type 2 diabetes and insulin resistance. Hebei Medicine 26 (4), 292–293.

Roy, T., 2012. Insulin resistance and type 2 diabetes. Diabetes 61 (4), 778–779.

Rea, S., James, D.E., 1997. Moving glut4: the biogenesis and trafficking of glut4 storage vesicles. Diabetes 46 (11), 1667–1677.

Stumvoll, M., Goldstein, B.J., Haeften, T.W., 1990. Type 2 diabetes: principles of pathogenesis and therapy. Lancet 365 (9467), 1333–1346.

Saltiel, A.R., Olefsky, J.M., 1996. Thiazolidinediones in the treatment of insulin resistance and type II diabetes. Diabetes 45 (12), 1661–1669.

Schinner, S., Scherbaum, W.A., Bornstein, S.R., Barthel, A., 2005. Molecular mechanisms of insulin resistance. Diabet. Med. 22 (6), 674–682.

Takenaka, H., Horiba, M., Ishiguro, H., Sumida, A., Hojo, M., Usui, A., et al., 2009. Midkine prevents ventricular remodeling and improves long-term survival after myocardial infarction. Am. J. Physiol-Heart C. 296 (2), H462–H469.

Taguchi, H., Endo, T., Yosioka, I., Iitaka, Y., 2008. The revised stereostructure of patrinoside X-Ray crystallographic analysis. Chem. Pharm. Bull. 27 (5), 1275–1276.

Woodruff, M.L., Rajala, A., Fain, G.L., Rajala, R.V., 2015. Effect of knocking down the insulin receptor on mouse rod responses. Sci. Rep-uk. 5, 7858.

Wu, Y., Lu, H., Yang, H., Li, C., Sang, Q., Liu, X., et al., 2016. Zinc stimulates glucose consumption by modulating the insulin signaling pathway in L6 myotubes: essential roles of Akt-GLUT4, GSK3$\beta$and mTOR-S6K1. J. Nutr. Biochem. 34, 126–135.

Xu, X.Q., Saadeldeen, F.S.A., Xu, L.T., Zhao, Y.Y., Wei, J.F., Wang, H.D., et al., 2019. The Mechanism of phillyrin from the leaves of *Forsythia suspensa* for improving insulin resistance. BioMed Res. Int. https://doi.org/10.1155/2019/3176483.

Zhang, T.B., Sun, M.L., 1997. Effects of V_2O_5 on proliferation and differentiation of limb bud cells of rat. Chin. Dev. & Reprod. Biol. Socs. 6 (2), 39–45.

Zhang, L., Xie, P., Wang, J., Yang, Q., Fang, C., Zhou, S., et al., 2010. Impaired peroxisome proliferator-activated receptor-gamma contributes to phenotypic modulation of vascular smooth muscle cells during hypertension. J. Biol. Chem. 285 (18), 13666–13677.

Zhu, Y.W., Song, C., Huo, H.R., Wang, L.F., Zhu, Y.T., Huang, Y.N., et al., 2015. Research of traditional Chinese medicine in treating type II diabetes and insulin resistance. World Chinese Medicine 10 (1), 135–137.